# Anisotropic High Cycle Fatigue Behavior and Related Crack Initiation mechanisms in forged steel

E. Pessard[1], F. Morel[1], A. Morel[1], D. Bellett[1]
[1]*Arts et métiers ParisTech, Laboratoire Procédés Matériaux Instrumentation Centre Angers, 49 035, Angers Cedex*

**Abstract:**
This work deals with the anisotropic fatigue behaviour of the Bainitic Steel Metasco®MC and aims at improving the fatigue criteria used for the design of forged components (e.g. automobile suspension arms). This material contains elongated manganese sulphide (MnS) inclusions oriented parallel to the rolling or forging direction. Specimens with different orientations relative to the rolling direction have been tested in fatigue under push-pull uniaxial loads.
The influence of "inclusion clusters" is clearly demonstrated via observation of the failure surfaces. Experiments show that the anisotropic fatigue behaviour is due to a change in the crack initiation mechanism. At 0°, when the inclusions are parallel to the applied stress, micro-crack initiation is controlled by the material matrix. At 90°, elongated manganese-sulphide inclusion clusters are at the origin of crack initiation and the fatigue strength drops significantly.
A statistical approach based on a competition between the 2 different crack initiation mechanisms is proposed. One mechanism is modeled by local elastic shakedown concepts and the other by linear elastic fracture mechanics. This approach leads to a Kitagawa type diagram and explain the anisotropy in the material. The approach developed in the of the weakest link theory to account for the loading mode, loading path and data scatter in High Cycle Fatigue.

## 1 Introduction

Forged components are recognized as having good mechanical properties, in particular in fatigue. This is mainly due to the microstructure induced by the forging process which leads to:

- the improvement of the material compactness,
- a finer and more homogeneous microstructure (e.g. a broken dendritic structure)
- fibering

The latter can result in considerable variation of the fatigue limit, depending on the fiber orientation. This variation has been reported as being 35% for 42CD4 steel [1] and 15% for a duplex stainless steel [2]
In order to correctly size a forged component in terms of fatigue, the thermo-mechanical history leading to the fibering orientation, the size and orientation of the grains or inclusions should be taken into account. Nowadays, process simulation software makes it possible to predict the fibering of a forged component [3].
Some high cycle fatigue models take into account the effect of the residual stresses, [4, 5] or the nature, the size and the orientations of the defects (or inclusions) with respect to the stress axis [3, 6, 7, 8, 9]. The objective of this work

is to propose a criterion adapted to anisotropic materials in fatigue that can take into account the strength of the material matrix and the effect of defects.

## 2 Material and experimental procedure

The material studied in this work is a Bainitic steel commercially referred to as Metasco®MC (25MnCrSiVB6) and is commonly used for the hot forging of automotive components. Its chemical composition is given in Table 1. The material is produced in the form of bars with a deformation ratio of about 15 and contains the following non-metallic inclusions (MnS, $Al_2O_3$, TiN and VN). The Ultimate Tensile Strength of the material is 1178 MPa, 1127 MPa and 1130 MPa for the 0°, 45° and 90° orientations respectively and the hardness is 318 HV in all three directions.

Table 1. Chemical Composition (weight %).

| Element | C | Mn | Si | Cr | S | Mo | V | Ti |
|---|---|---|---|---|---|---|---|---|
| Weight % | 0.255 | 1.30 | 0.9 | 0.8 | 0.075 | 0.075 | 0.185 | 0.025 |

Poles figures determined via EBSD on the residual austenite and ferrite shows that there is no crystallographic texture. Moreover, micrographic observations show that the ex-austenitic grains are equiaxed. These two observations show that if the fatigue behavior is anisotropic, it cannot be due to the microstructure of the material matrix.

Forty-five hour glass specimens for testing in uniaxial HCF were machined from rolled bars (diameter 80mm) in 3 different directions with respect to the rolling direction: parallel (0°), perpendicular (90°) and at 45 degrees (45°). All specimens were annealed at 525°C for one hour in a vacuum to eliminate residual stresses introduced via polishing or machining. Push Pull (R=-1) fatigue tests were performed in a servo-hydraulic Instron testing machine at a frequency of 25Hz. The fatigue limits were evaluated using the staircase method, at $2x10^6$ cycles. All tests were carried out at room temperature and pressure in air. Non-broken specimens from the staircase were re-tested at a higher stress level in order to estimate the slope of the Wöhler curve.

The fracture surfaces of all the tested specimens were examined using a Scanning Electron Microscope (SEM).

## 3 Experimental results

*Fatigue strength curves*

The fatigue strength at 2x106 cycles is highest for an orientation of 0° and lowest at 90° (see Figure 1 b)). In terms of the finite-life regime (i.e. for a stress level of 560 MPa) the average fatigue life is the same ($N=10^5$ cycles) for the 0° and 45° orientations, but is much lower for 90° ($N=2.10^4$ cycles) (see Fig. 1 a)). The coefficient of variation (COV=average fatigue limit value/ standard deviation) is similar for the 45° and 90° orientations; however it is twice as large for the 0° orientation (Table 2).

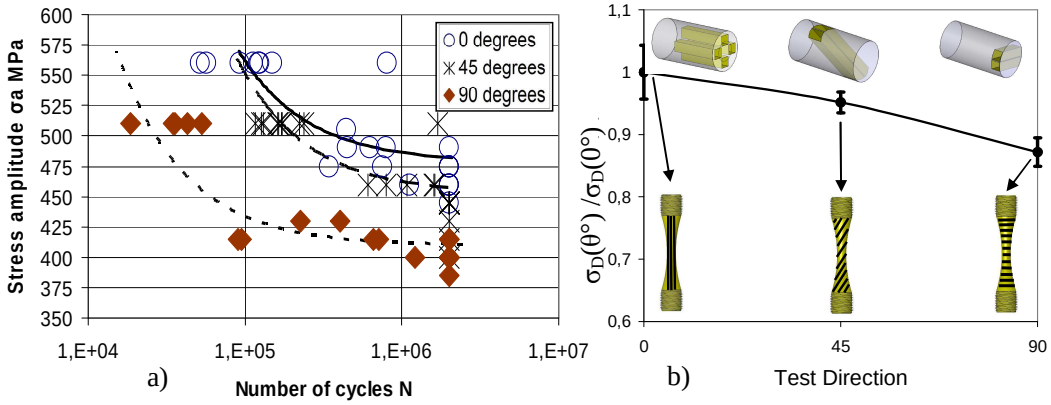


Figure 1: a)Wöhler curves for different specimen orientations with respect to the rolling direction, b) Push-Pull Fatigue Limit (Normalised by the 0° value) as a function of the test direction.

Table 2. Average Value and Standard Deviation for the fatigue Push Pull test in each direction for the Metasco®MC

| Test direction (Degrees) | Average fatigue limit Value (MPa) | Standard Deviation | COV |
|---|---|---|---|
| 0 | 476 | ±20 | 0.042 |
| 45 | 453 | ±8 | 0.018 |
| 90 | 415 | ±11 | 0.026 |

*Observations of the Fatigue Mechanism*

For the 0° specimens, where the inclusions are parallel to the applied stress, cracks initiate in the material matrix (i.e. bainitic microstructure), typically at 45 degrees to the loading direction. This corresponds to the "classical" fatigue crack initation mechanism in which micro cracks form on a critical plane (or plane of greatest shear stress amplitude), in the weakest and/or most favourably orientated grains. Both in-situ observation of the specimen surfaces (Fig. 2b)) and SEM observations of the failure surfaces (Fig. 2a)) show that the crack initiation sites are not associated with the presence of non-metallic inclusion.

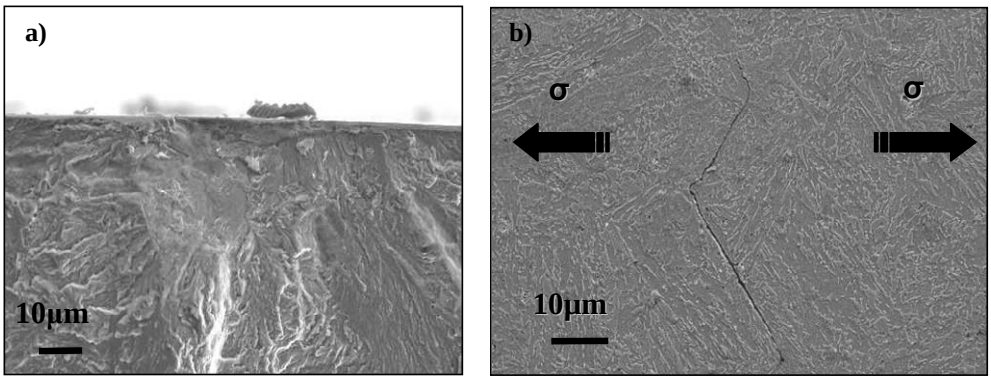

Figure 2: Observation at 0° a) Fracture surface initiation site without inclusions b) Crack path in the bainitic microstructure on a specimen surface.

For the 90° specimens, observations show that there are two different fatigue crack initiation mechanisms that can occur. These are:

1. Crack initiation in the material matrix as discussed above for the 0° case.
2. Crack initiation from Manganese Sulphide (MnS) inclusion cluster. The inclusion type was verified by EDS (Energy Dispersive Spectrometry). It can be seen from Fig. 3 that these soft, non-metallic inclusions are elongated in the direction of rolling. They have an average diameter of 2µm and a length of 100µm up to several mm. However, more importantly, these inclusions are grouped into bands or clusters (See Fig 3b)). It is these cluster that can have a detrimental effect of the fatigue strength.

For the 90° orientation, final failure of the specimens is determined via competition between these two mechanisms.

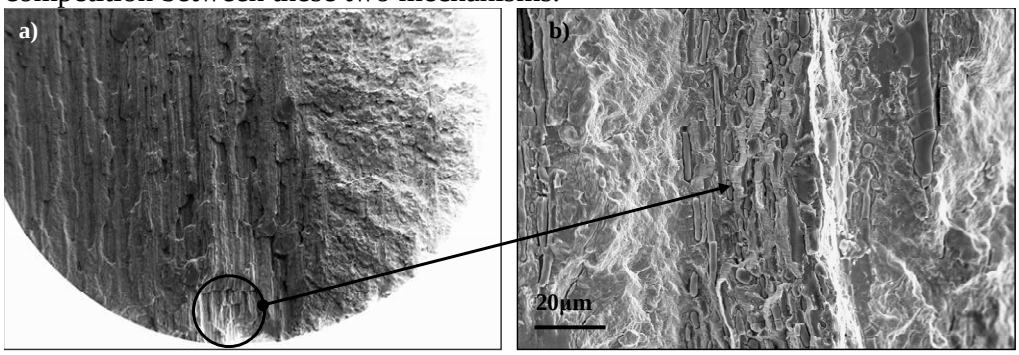


Figure 3: Observation at 90° a) Rupture surface b) MnS Inclusion band

Figure 4 shows an SEM image of the surface of a 90° specimen taken during a interrupted fatigue test. In this image both initiation mechanisms, discussed above, can be visualised. At the bottom right of the picture a crack, initiated in the material matrix can be seen (i.e. Mechanism 1). This crack is at 45° to the loading direction. A second crack can be noted at the top left, which initiates from an inclusion cluster and is oriented at 90° to the loading direction (i.e. Mechanism 2). In Fig 4 the inclusions are darker and an inclusion cluster, perpendicular to the image or specimen surface, can be seen at the top left of the picture. Note that none of the observed cracks that initiated via this mechanism occurred at a single isolated MnS inclusion, but due to a band or cluster of inclusions. SEM images of the failure surfaces show that the failure surface is very rough and the long MnS bands are easily identified (see Fig. 3 a)). In this case the initiation is not localized in just one site. This type of fracture surface would be caused by several cracks originating from several inclusions bands, propagating and joining each other to create the final crack (Fig. 3 b).

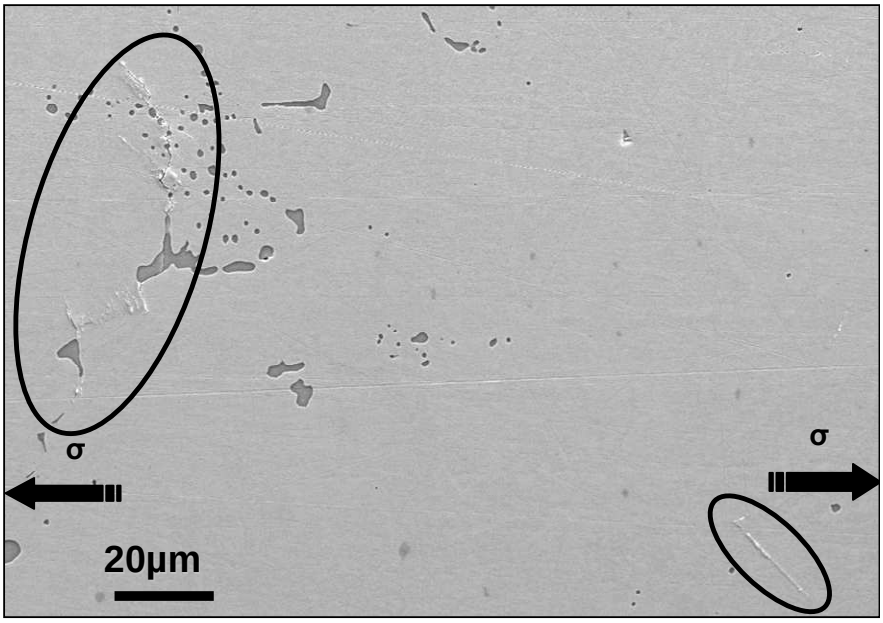


Figure 4: Surface observation on a 90° specimen, highlighting the competition between two mechanisms: initiation from inclusion clusters and from the bainitic matrix

For the specimens oriented at 45° to the rolling direction the situation is not as clear. In terms of surface observations, all of the cracks appeared to initiate in the metal matrix (at 45° to the loading direction). However, SEM analysis of the failure surface revealed that some initiation sites are centered on an inclusion cluster. Hence, it is assumed that, like above, the final failure of the specimens orientated at 45° is determined via competition between the two, previously discussed mechanisms.

All these observations show that the orientation of the specimen, with respect to the rolling direction, greatly influences the fatigue behavior. At 0° the cracks are initiated in the material matrix and both the fatigue limit and the standard deviation are high. At 90°, the MnS clusters appear on the fracture surface as bands, which govern the fatigue behavior and further decrease the fatigue limit and the standard deviation.

## 4 A probabilistic multiaxial fatigue criterion reflecting the competition between mechanisms

In the literature, very often two different approaches coexist and try to model the same behavior. In terms of fatigue, one common approach is to model the local plasticity in a grain (surrounded by an elastic matrix) [4, 5, 10]. Other popular approaches are based on Fracture Mechanics and describe crack growth [6, 9]. Both of these have their advantages and limitations, and in the opinion of the authors the first is the most appropriate to model the first crack initiation mechanism, discussed above, whereby micro-cracks occur in the material matrix. On the other hand, a fracture mechanics approach is better suited to the second mechanism in which cracks are controlled by the inclusion cluster. An additional

complication when trying to choose a modelling approach is crack size. It is very difficult to build a single model that takes into account, at the same time, both very small cracks and long cracks. Because as the crack size becomes small, the local plasticity mechanism becomes dominant.
In this work, it was decided not to make a choice, but to introduce a competition between the two possible mechanisms. That is, it is assumed that both mechanisms co-exist, however one gains dominance over the other and leads to final failure. The approach developed here uses two different models combined by a probabilistic calculation.
The first mechanism takes into account the local plasticity and is based on the shear stress. The local plasticity is considered responsible for crack initiation in the matrix. The second mechanism is governed by the normal stress and considers crack growth. In this case, the inclusion clusters are considered to be cracks.

**Modeling of mechanism 1**

**In the material matrix**, the fatigue behavior is assumed to be controlled by the concept of elastic shakedown. That is, the fatigue limit is defined as the loading level at which, all (isolated) plastically deforming grains, on the mesoscale, re-establish their purely elastic cyclic comportment.
Papadopoulos [5] showed that the amplitude of the macroscopic resolved shear stress $T_a$ acting on a glide system defined by three angles (φ,θ,ψ) in a grain can be used as an indicator of the possibility of achieving an elastic shakedown state, in a grain. The random nature of the local resistance to crack initiation is introduced through a Weibull distribution [5, 10] of the mesoscopic elastic shakedown threshold. The weakest link theory is then applied via a spatial integration, carried out on all the possible glide systems, to take into account the probability of crack initiation in all possible systems. The failure probability of an elementary reference volume is therefore:

$$P_{F1} = 1 - \exp\left[ -\frac{1}{D_0} \int_{\varphi=0}^{2\pi} \int_{\theta=0}^{\pi} \int_{\psi=0}^{2\pi} \left( \frac{T_a(\varphi,\theta,\psi)}{T_{01} \Big/ \left(1 + k \frac{\Sigma_{H,a}}{\mathscr{T}_a}\right)} \right)^{m_1} \sin\theta \, d\psi \, d\theta \, d\varphi \right] \quad (1)$$

Where $D_0$ is a material parameter, $T_{01}$ is a scale factor that depends on the average fatigue limit of the material matrix. k is a material parameter and reflects the sensitivity to the hydrostatic stress $\Sigma_{H,a}$.

$\mathscr{T}_a$ is the maximum shear stress amplitude:

$$\mathscr{T}_a = \max_{\varphi,\theta,\psi} \{T_a(\varphi,\theta,\psi)\} \quad (2)$$

$m_1$ is the Weibull exponent [11] and reflects the experimental scatter associated with the mechanism occurring in the matrix.

**Modeling of mechanism 2**

In the following **the inclusion bands** (see Fig 3a)) are considered to be pre-existing cracks. The fatigue limit is therefore defined by a condition of non-propagation. The main driving force for crack growth is assumed to be the normal stress acting on a given material plane. As per the previous case and for sake of simplicity the randomness of the propagation threshold related to the presence of a crack will be introduced through a Weibull distribution.

$$P_{F2} = 1 - \exp\left[ -\frac{1}{D_{02}} \int_{\varphi=0}^{2\pi} \int_{\theta=0}^{\pi} \left( \frac{\sigma_a(\varphi,\theta)}{\sigma_{02}(f,\theta)} \right)^{m_2} d\theta d\varphi \right] \quad (3)$$

The double integration takes into account the propagation potential in all the planes defined by $\underline{n}$. The exponent $m_2$ governs the scatter while the scale factor, $\sigma_{02}$, influences the mean value of the distribution. $\sigma_a(\varphi,\theta)$ is the amplitude of the normal stress applied on a plane defined by $\underline{n} = \begin{pmatrix} \sin\theta\cos\varphi \\ \sin\theta\sin\varphi \\ \cos\theta \end{pmatrix}$

$$\sigma_a(\varphi,\theta) = \underline{n}.\underline{\underline{\sigma_a}}.\underline{n} \quad (4)$$

For a Weibull distribution the scale factor $\sigma_{02}$ depend on the average fatigue limit, the exponent $m_2$ and the geometrical factor $\Phi(f,\theta)$.

$$\sigma_{02}(f,\theta) = \frac{K_{th}}{\Gamma(1 + 1/m2)\Phi(f,\theta)\sqrt{\pi a}} \quad (5)$$

$\Phi(f,\theta)$ is the complete elliptical integral of the second kind for an elliptical shaped crack, and depends on the crack aspect ratio. $f$ is a parameter used to define the fibering orientation. With this expression, at 0° the inclusion clusters are considered to be circular (penny shaped) cracks and at 90° as through cracks. In order to simplify equation (3) the following definition is used:

$$J_{m_2}(f) = \int_{\varphi=0}^{2\pi} \int_{\theta=0}^{\pi} \left( \frac{\sigma_a(\varphi,\theta)}{\Sigma_a \Phi(f,\theta)} \right)^{m_2} d\theta d\varphi \quad (6)$$

With $$\Sigma_a = \max_{\varphi,\theta}\{\sigma_a(\varphi,\theta)\} \quad (7)$$

And $$\Sigma_{02} = \frac{K_{th}}{\Gamma(1 + 1/m2)\sqrt{\pi a}} \quad (8)$$

Hence: $$P_{F2}(f) = 1 - \exp\left[ -\frac{\Sigma_a{}^{m_2} J_{m_2}(f)}{\Sigma_{02}{}^{m_2}} \right] \quad (9)$$

**A probabilistic combination** of the two previously defined failure probabilities is proposed below. Based on the observations of the crack initiation mechanisms (Fig. 4) the survival probability of the entire component is deduced from the product of the two survival probabilities relative to the two mechanisms observed.

$$1-P_F(f)=(1-P_{F1})(1-P_{F2}(f)) \tag{10}$$

In the case of push pull loading equation 10 can be written as:

$$\Sigma_{d(a)}\left(1+\frac{\sum_{d(a=0)}^{m_1} J_{m_2}(f)}{\ln\left(\frac{1}{1-P_f}\right)\Sigma_{02}^{m_2}}\Sigma_{d(a)}^{(m_2-m_1)}\right)^{1/m_1}=\Sigma_{d(a=0,P_f)} \tag{11}$$

This relation leads to a Kitagawa type diagram giving the fatigue limit as a function of the average crack size. When the crack size is small, local plasticity controls the fatigue behavior, when the crack is long, LEFM and the normal stress are appropriate for predicting crack growth. Between these two domains competition occurs (see Fig 5). An important feature of this novel approach is that it is possible to draw the curves for different failure probabilities and hence explain the evolution of the standard deviation with the average crack size (Fig.5).

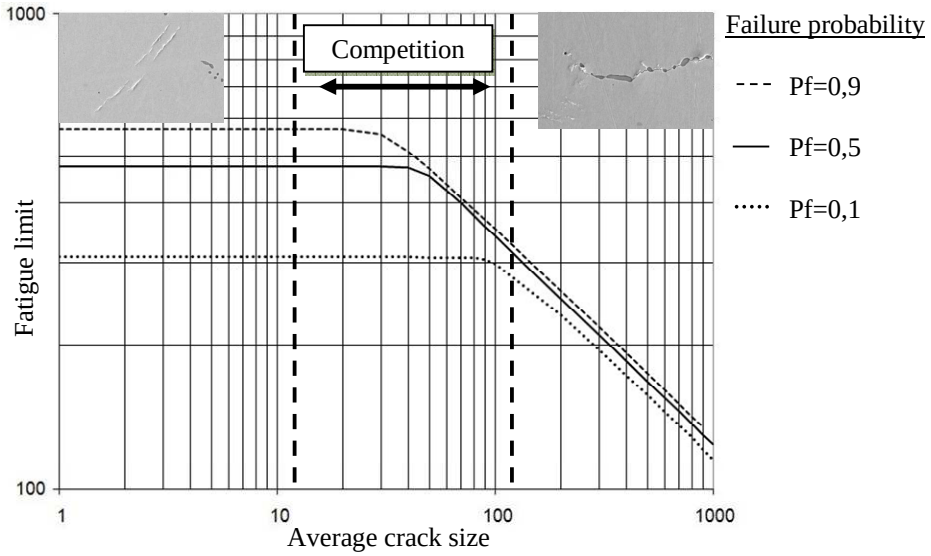


Figure 5: Kitagawa type diagram with different failure probabilities, $K_{th}$=4MPa.m$^{1/2}$, $\sigma_D$(a=0)=475MPa, $m_1$=5 and $m_2$=30

Note that in Eq. (11), the evolution of $\Sigma_{d(a)}$ depends on $J_{m_2}(f)$ or the fibering orientation. Consequently, a curve can be plotted on the Kitagawa diagram for each fibering orientation (see Fig. 6). From this diagram, for a given crack size it is possible to predict the fatigue limit for each fibering orientation. For the Metasco®MC steel, the average inclusion cluster size is about 32µm and the model predicts a fatigue limit for a push-pull loading of 471MPa, 465MPa and 415MPa respectively for the orientation at 0°, 45° and 90°.

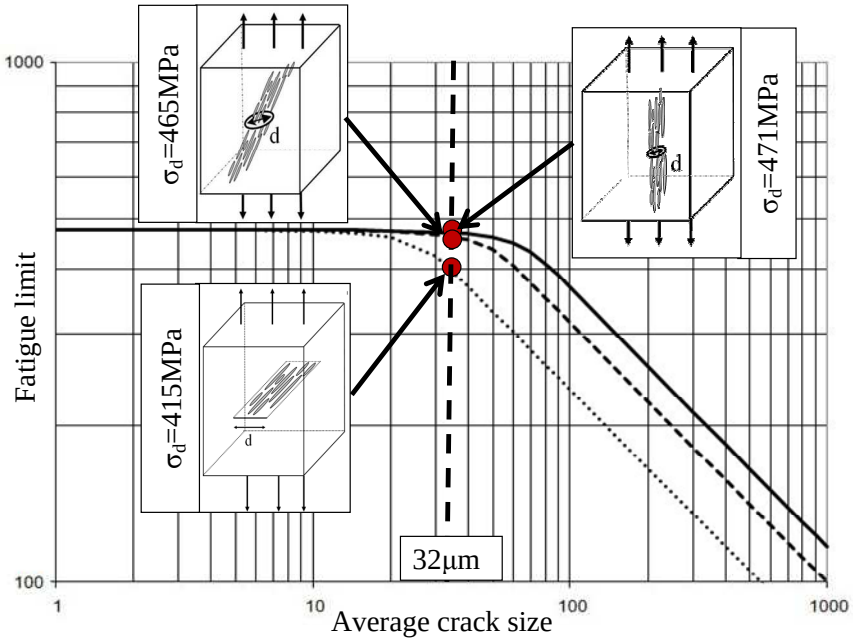


Figure 6: Kitagawa type diagram for each orientation

## 5 Conclusion

The forged bainitic steel Metasco®MC is found to have anisotropic fatigue behaviour due to a change in the crack initiation mechanism.

For a fibering at 0° the fatigue behaviour is controlled by local plasticity in the material matrix, the fatigue limit and the standard deviation are high.

For a fibering oriented at 90°, competition between two crack initiation mechanisms occurs: initiation from the material matrix and from elongated manganese sulphide clusters. The fatigue limit and the standard deviation are lower.

A probabilistic model that takes into account the competition between the two mechanisms is proposed. It leads to a probabilistic kitagawa type diagram that can explain the experimental evolution of the fatigue limit and the scatter with the fibering orientation for a push-pull loading test.

## 6 Acknowledgments

This work is being performed within the ANR (National Research Agency) Optiforge project, in a partnership including several industrial (Ascoforge, Ascometal, Cetim, PSA, Setforge, Transvalor) and academic (INSA Lyon, ENSMP-CEMEF, Arts et Métiers PARISTECH Angers) institutions.

## 7 References


[1] J.Y. Berard, K. Dang Van and G. Baudry, influence de l'anisotropie sur le comportement en fatigue multiaxiale d'un acier de construction mécanique, IRSID, Technical Note No RI 93 062 (1993).

[2] A.Mateo, L. Llanes, N. Akdut, J Stolarz and M.Abglada, Anisotropy effects on the fatigue behaviour of rolled duplex stainless steels, Int. J. of Fatigue Res **25** (2003) 481-488.

[3] Y. Chastel, N. Caillet, P.O. Bouchard, Quantitative analysis of the impact of forging operations on fatigue properties of steel components, Journal of Materials Processing Technology Res 177 (2006) 202-205.

[4] K. Dang van, Macro–micro approach in high-cycle multiaxial fatigue. In: McDowell DL, R. Ellis, editors. Proceedings of advances in multiaxial fatigue, ASTM STP 1191 (1993) 120–130.

[5] I.V. Papadopoulos, Fatigue limit of metals under multiaxial stress conditions: the microscopic approach, Commission of the European Communities, Joint Research Center, 1993.

[6] Y. Murakami, S. Beratta, Small Defects and Inhomogeneities in Fatigue Stregnth: Experiments, Model and Statistical Implications, Kluwer Academic Publishers, 1999.

[7] A. Ekberg, and P.,Sotkovski. Anisotropy and rolling contact fatigue of railway wheels. International Journal of Fatigue (2000) 29-43.

[8] T. Makino, The effect of inclusion geometry according to forging ratio and metal flow direction on very high-cycle fatigue properties of steel bars. International Journal of Fatigue (2007) 1409-1418.

[9] E. Thieulot-Laure, S. Pommier, S. Fréchinet, A multiaxial fatigue failure criterion considering the effects of defects, International journal of Fatigue Res 29 (2007) 1996-2004.

[10] F. Morel and N. Huyen, Plasticity and damage heterogeneity in fatigue, Theoretical and Applied Fracture Mechanics Res 49 (2008) 98-127.

[11] Weibull W. A statistical distribution function of wide applicability. Journal of Applied Mechanics Res 18(3) (1951) 293-297.